Korean J. Chem. Eng., 19(1), 167-174 (2002)

Studies on the Preparation of C/SiC Composite as a Catalyst Support by CVI in a Fluidized Bed Reactor

Sung-Joo Lee, Mi-Hyun Kim, Yong-Tark Kim and Gui-Yung Chung†

Department of Chemical Engineering, Hongik University, 72-1 Sangsu-Dong, Mapo-Ku, Seoul 121-791, Korea
(*Received 1 February 2001 • accepted 30 July 2001*)

Abstract—In this research, in order to improve the mechanical strength and oxidation resistance of a catalyst support, we studied the formation of SiC layer on the pore surfaces of activated carbons by permeating and depositing SiC from a reaction between hydrogen and dichlorodimethylsilane (DDS). The porous structure should be kept during deposition. A fluidized bed reactor and activated carbons of size of 20-40 mesh were used. By studying characteristics of deposits under various deposition conditions, we confirmed that the best conditions of manufacturing catalyst support are a lower pressure and a lower concentration. In this work, at the conditions of 5 torr of total pressure and 3% of DDS concentration, during the 10 hr processing time, deposition occurred on the pore walls before plugging pores. The results from the mathematical modeling were compared with the experimental results.

Key words: Fluidized Bed Reactor, CVI, Ceramic Composites, Silicon Carbide, Catalyst Support

INTRODUCTION

Composites of activated carbon reinforced with silicon matrix (C/SiC) have received considerable attention for high-temperature structural applications because of their superior strength, fracture toughness, and abrasive properties. Compared with carbon/carbon composite (C/C), C/SiC composites exhibit higher mechanical properties and oxidation resistance. So far, four kinds of processing techniques have been developed for fabrication of the composites: slurry infiltration and hot-pressing, polymer conversion, silicon melt infiltration, and chemical vapor infiltration [Sea et al., 1995].

The technique of slurry infiltration and hot-pressing, which has a short processing time and is inexpensive in practice, has been used most effectively for glass and glass-ceramic matrix systems. In refractory matrix systems (e.g. SiC), it is less effective because of the absence of viscous flow. The problem that arises is fiber degradation or damage resulting from mechanical contact with the refractory particles. The advantages of polymer conversion are as follows: great composition homogeneity, the potential for forming unique multiphase matrix, and ease of infiltration of forming. The principal disadvantages of this technique are high shrinkage and low yield of polymer during pyrolysis. Silicon melt infiltration method is based on a polymer pyrolysis subsequently followed by the infiltration of silicon melt. However, there are some obstacles in applying this method to ceramic: fiber damaging and chemical reactions at infiltration temperature. Chemical vapor infiltration (CVI) was developed as an extension of the well-established chemical vapor deposition and has been in commercial production. The primary advantage of this method is a uniform coating of tailored compositions for multi-layer at a relatively low temperature (900-1,100 °C).

In general, deposition of silicon carbide was obtained from the reaction between hydrogen and methylchlorosilanes. Among them methyltrichlorosilane (CH_3SiCl_3) has been studied many times [Kim et al., 1993; Kobayashi et al., 1976]. In this research, dichlorodimethylsilane [DDS, $(CH_3)_2SiCl_2$] was used. Silicon carbide obtained from the reaction between DDS and H_2 was infiltrated and deposited on the pore walls of activated carbon. CVI was done in a fluidized bed reactor to obtain a uniform deposition.

The objective of the current work is to confirm the optimum conditions for deposition by doing experiments with different pressures and concentrations in the reactor. Also, effects of parameters for deposition were observed by calculating amounts of deposition, concentration distributions, and final porosities, etc. with a mathematical modeling and compared with experimental results. The concentrations of reactant gas, i.e., DDS, in the reactor and in activated carbons were calculated. Changes of dimensions of pores in activated carbons with reaction time were predicted.

In the present research, deposition reactions were carried out in a fluidized bed reactor. The reaction pressure and the concentration were changed. To obtain a uniform deposition on the walls of pores, the rate of diffusion must be faster than that of deposition. These conditions are low pressures and low concentrations [Naslain, 1990; Naslain et al., 1983; Van den Brekel et al., 1981]. The amount of deposition, the surface area and the porosity of activated carbons before and after deposition reactions were measured by using TGA, BET surface analyzer and a mercury porosimeter.

Mathematical modeling was performed to describe the deposition on the pore walls. Experimental results, such as amount of deposition, surface area, and porosity, were compared with the modeling results. It is expected that the results of this research can suggest proper experimental conditions for the CVI processes in the fluidized bed reactor [Hwang et al., 1999].

EXPERIMENTAL

The experimental setting, shown in Fig. 1, consists of three parts: the supply part of gases, the furnace, and the discharge part of product gases. The supply part of gases consists of cylinders of H_2 and

†To whom correspondence should be addressed.
E-mail: gychung@hongik.ac.kr

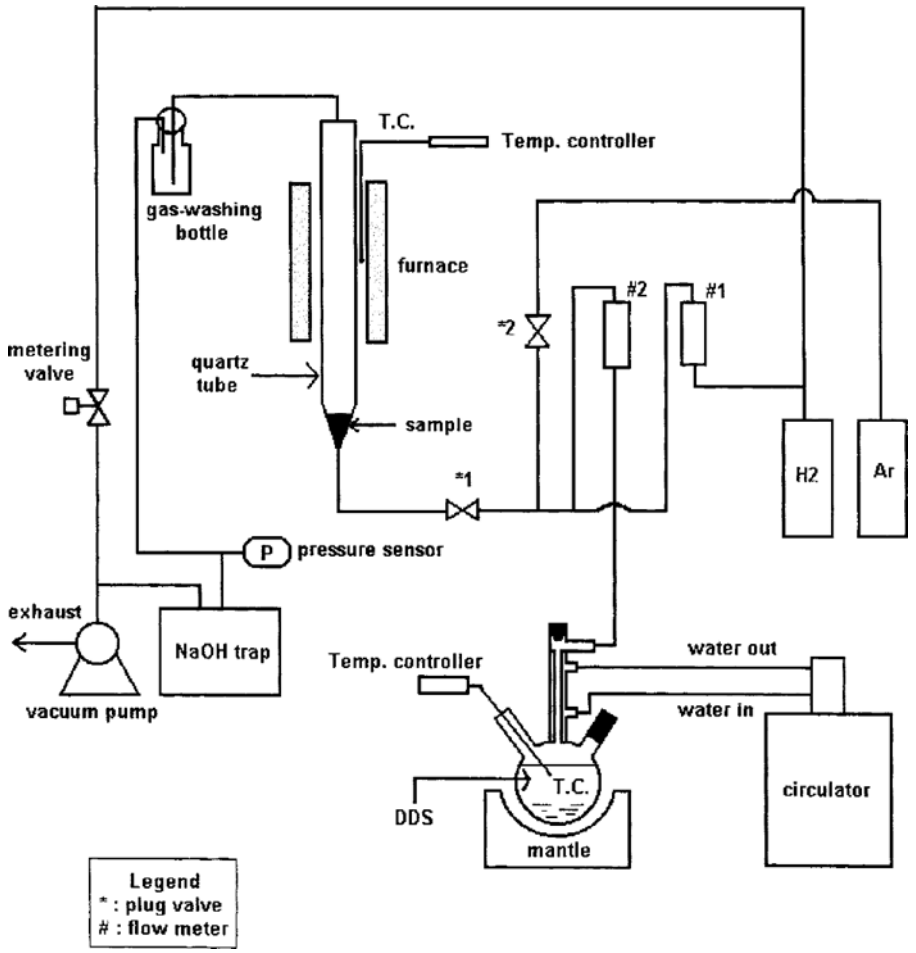

Fig. 1. Schematic diagram of the experimental apparatus.

Ar, a flow meter, a flask with the reactant, DDS. The reactor was a vertical quartz tube whose the inside diameter and the length is 2.5 cm and 1 m, respectively. A thermocouple was mounted in it. The discharge part of product gases consists of a vacuum gauge, a NaOH trap, and a vacuum pump.

In this research, activated carbons of 4-12, 12-20, 20-40 mesh were used. DDS was supplied by the carrier gas, H_2. The reaction temperature was 950 °C and the flow rate was 500 ml/min. This flow rate was adjusted to position the fluidized samples at the heating zone which was found before fluidization reaction by using a thermocouple. DDS concentrations of 3, 5, 7, and 9% and reaction pressures of 7, 10, 20, and 40 torr were used.

The system was evacuated first. Then, while H_2 was supplied, the furnace temperature was raised. After the reactor temperature reached a reaction temperature, DDS was supplied. The flow rates of H_2 and DDS were maintained with flow meters. When the reaction finished, the supply of DDS was stopped and the samples were taken out from the reactor.

After the deposition reaction, the amount of deposition, the pore size distribution, and the surface area were measured with TGA (Du pont 951), porosimeter (Poresizer 9320), and BET (Micromeritics Co. ASAP-2000), respectively.

MATHEMATICAL MODELING

1. Model Development

Mathematical modeling to describe the deposition on the pore walls of activated carbons was performed by solving differential equations of mass balance including the deposition reaction and an equation of changes of pore diameter with time.

Schematic diagrams of the reactor and an activated carbon for the mathematical modeling are shown in Fig. 2. The reaction gas flows from the bottom to the top of the reactor and diffuses into pores of an activated carbon. DDS gas flows in the z-direction and diffuses in the r-direction of the reactor and in the r'-direction of an activated carbon.

The radius of the reactor is R_o and the floating height of carbons is H. The diameter of an activated carbon is r_o and the pore diameter is d_o. Reactant concentrations in the reactor and in the pores of activated carbons are C_A and $C_{Ar'}$, respectively.

The following assumptions are used. All activated carbons have a spherical shape with the same radius. Pores in activated carbons are assumed to have a conical shape whose bottom is the open entrance for gas. It is assumed isothermal inside the reactor regardless of the position.

Reactant gases in the reactor flow by convection in the z-direction and by diffusion in the z- and the r-directions. Deposition occurs on the surface of samples and on the walls of the reactor. There is only diffusion in the r'-direction from the surface to the

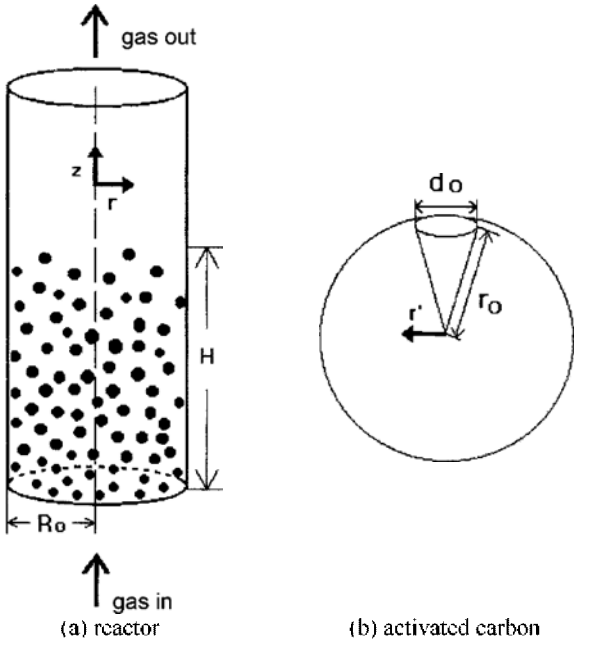

Fig. 2. Schematic diagrams of the FB-CVI reactor and an activated carbon used in the simulation.

center of an activated carbon. Pyrolysis reaction of DDS is assumed as the first order reaction [Sugiyama and Kurisu, 1989]. Positions of fluidized particles are assumed to be fixed.

Deposition occurs on the inside wall of the reactor and on the walls of pores of activated carbons. Because of many pores in an activated carbon, deposition on the outside surface of an activated carbon is neglected before pores are plugged. As deposition occurs on walls of pores, diameters of pores decrease. After pores are plugged, there is no more deposition inside activated carbons. Therefore only the deposition on the outside surface of activated carbons is considered.

2. Mass Balance

Even though dimensions of samples change continuously, the changes are very small compared to those of concentration distributions. So a pseudo steady state is assumed.

Mass balances of the reactant gas, DDS, in the reactor include convection, diffusion, and depositions on the reactor wall and on the surfaces of activated carbons. Here the surfaces of activated carbons mean the outside surface of the spherical carbon and the pore walls in the carbon.

The mass balance equations of DDS before pore entrances are plugged are as follows.

$$-\frac{\partial N_{Az}}{\partial z}-\frac{1}{r}\frac{\partial}{\partial r}(rJ_{Ar})-F\frac{\pi d^2}{4}N_p J_{Ar}|_{r'=r_0,z,r}$$
$$-F\left(4\pi r_0^2-\frac{\pi d^2}{4}N_p\right)k_r C_A=0 \quad (1)$$

b.c.1 at $z=0$, $C_A=C_{A_0}$ (2)

b.c.2 at $z=H$, $\frac{\partial C_A}{\partial z}=0$ (3)

b.c.3 at $r=0$, $\frac{\partial C_A}{\partial r}=0$ (4)

b.c.4 at $r=R_0$,

$$-\frac{1}{2}\frac{\partial}{\partial z}N_{Az}+\frac{1}{\Delta r}(J_{Ar}|_{R_0}-k_r C_A)$$
$$-\frac{F\pi d^2}{8}N_p(J_{Ar'}|_{r'=r_0,z,r}-k_r C_A)-2F\pi r_0^2 k_r C_A=0 \quad (5)$$

Here, $N_{Az}=v_z C_A+J_{Az}$ and $J_A=-D_e\nabla C_A$. F is the number of activated carbons in a unit volume. N_p is the number of pores in an activated carbon. N_p is decided in such a way that the single pore volume multiplied by N_p becomes the pore volume in an activated carbon measured experimentally.

Diffusion into activated carbons and deposition on the surface of activated carbons were included in the mass balance Eq. (1). The system from the entrance to the floating height (H) of activated carbons was considered for numerical modeling. A symmetrical boundary condition was used at the center of the reactor (r=0) and the boundary condition at the reactor wall ($r=R_0$) is shown in the Eq. (5).

The mass balance of DDS after pores are plugged is as follows:

$$-\frac{\partial N_{Az}}{\partial z}-\frac{1}{r}\frac{\partial}{\partial r}(rJ_{Ar})-F4\pi r_s^2 k_r C_A=0 \quad (6)$$

Deposition inside activated carbons does not occur any more after pores are plugged. Only deposition on the outside surface of activated carbons occurs so that the sample radius increases; r_s is the sample radius changing with reaction time. Boundary conditions of Eq. (6) are same as those of Eq. (1) except the following boundary condition at $r=R_0$.

$$-\frac{1}{2}\frac{\partial N_{Az}}{\partial z}+\frac{1}{\Delta r}J_{Ar}|_{R_0}-2F\pi r_s^2 k_r C_A-\frac{1}{\Delta r}k_r C_A=0 \quad (7)$$

The mass balance equation of DDS inside activated carbons is as follows:

$$-\frac{1}{r'^2}\frac{\partial}{\partial r'}(r'^2 J_{r'})-\Omega k_r C_{Ar}=0 \quad (8)$$

b.c.1 at $r=0$, $\frac{\partial C_{Ar}}{\partial r}=0$ (9)

b.c.2 at $r=r_0$, $C_{Ar}=C_A$ (10)

Here, Ω is the surface area per unit volume of an activated carbon and r_0 is the radius of an activated carbon. Diffusion in the r'-direction and deposition reaction on pore walls are included in the balance equation.

The effective diffusion coefficient, D_{ep}, in the pores of activated carbons is obtained as follows:

$$D_{ep}=\varepsilon_p^2 D_{mk} \quad (11)$$

As diameters of pores decrease due to deposition, the porosity (ε_p) changes; therefore, D_{ep} changes.

Because pores are very small, Knudsen diffusion is important at a high temperature and a low pressure. Therefore D_{mk} is obtained by combination of the molecular diffusion coefficient and the Knudsen diffusion coefficient. The molecular diffusion coefficient D_m, is calculated using the Chapman-Enskog equation [Cho et al., 1996]. Knudsen diffusion coefficient, D_k, is calculated using the following

equation.

$$D_k = 5.82 \times 10^{-7} R \left(\frac{T}{M_A}\right)^{1/2} \quad (12)$$

Here, T [K] is temperature, M_A [g/mol] is molecular weight of DDS, R [cm] is the radius of pores.

After concentration profiles are calculated using mass balance equations of DDS, changes of the pore diameter, the amounts of deposition, and the surface area are calculated.

The shape of pores in an activated carbon is assumed as a conical shape of which the entrance diameter is d_0 and the height is same as the radius of an activated carbon, r_0. The number of pores in an activated carbon is assumed constant. Changes of pore diameter, d, with reaction time are calculated as follows:

$$\frac{dd}{dt} = -\frac{2qM_m k_r C_A}{\rho_m} \quad (13)$$

Here, q is the number of SiC molecules obtained from one molecule of reactant, DDS. Here, it is one. M_m and ρ_m are the molecular weight and the density of SiC.

Radius of an activated carbon, r_c, changes with time after pores are plugged.

$$\frac{dr_c}{dt} = \frac{qM_m k_r C_A}{\rho_m} \quad (14)$$

The amount of deposition, W, and the area per unit volume of the reactor, S, are calculated as follows:

$$W_{z,r} = \sum_{k=1}^{N} \frac{\pi(d_0^2 - d^2)}{4} \rho_m \Delta r N_p \quad (15)$$

$$S = \frac{dN_p}{4r'^2} \quad (16)$$

After pores are plugged, the deposition on the outside surface of activated carbons is included.

$$W_{z,r} = \sum_{k=1}^{N} \frac{\pi(d_0^2 - d^2)}{4} \rho_m \Delta r N_p + \frac{4}{3}\pi(r_c^3 - r_0^3)\rho_m \quad (17)$$

Porosity of an activated carbon is calculated from the following equation.

$$\varepsilon_p = \varepsilon_{p,0} - \frac{(d_0^2 - d^2) \cdot N_p}{16r'^2} \quad (18)$$

3. Calculation Procedure

Equations are made dimensionless by using a dimensionless concentration, (C_A/C_{Ao}), and a dimensionless length, (z/H) and (r'/r_c). z-, r-, and r'-directions are divided into 10 segments and the finite difference method is used.

The concentration profiles in the reactor are calculated first with Eq. (6). The concentration profile inside activated carbons is obtained by using the concentration at their surface which is calculated with Eq. (6). Calculations are repeated with an error range of 0.01%. Then changes of pore diameter, amount of deposition, surface area, and porosity are calculated. The same calculations at the next time step are repeated.

After pores are plugged, changes of the radius of an activated carbon (r_c) with reaction time are obtained with Eq. (14).

Reaction conditions used in the numerical modeling are shown in Table 1 and characteristics of activated carbons are shown in Table 2.

Table 1. Reaction conditions used in the experiment

Temperature	950 °C
Flow rate of the carrier gas at 25 °C	500 cm^3/min
Pressure	5, 7, 10, 20, 40 torr
Diffusion coefficient (D_m)	236 cm^2/min
Reactor radius (R_0)	1.1 cm

Table 2. Characteristics of activated carbons used in the experiment

	20-40 mesh
Sample weight (g)	0.406
Weight of one activated carbon (g)	0.0001
Radius of one activated carbon (cm)	0.04
Initial pore diameter (μm)	0.022
Surface area per unit weight (m^2/g)	114.8
Maximum floating height (cm)	22.1
Initial porosity	0.39
Number of activated carbons per unit volume, F (#/cm^3)	83.3

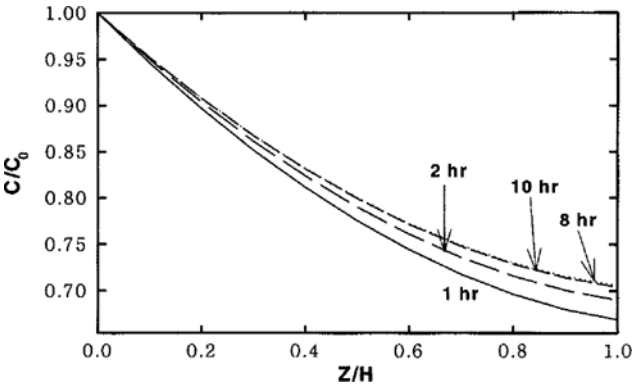

Fig. 3. Changes of dimensionless concentration of DDS in the gas phase with reaction time along the axis of cylinder. Reaction conditions: DDS 5%, 10 torr, 20-40 mesh activated carbon, k_r=10 cm/min.

RESULTS AND DISCUSSION

1. The Concentration Distribution and the Reaction Rate Constants

Changes of concentration distribution and sizes of pores with reaction time along the z-direction were predicted in Figs. 3 and 4 by mathematical modeling.

The concentration gradient along the z-direction in the reactor is influenced by diffusion and deposition reaction. Fig. 3 is the concentration distribution from the bottom to the floating height, H, along the z-direction in the reactor. The concentration distribution increases until about 8 hr, then it starts decreasing slowly. Because the surface area of pore walls is getting smaller until 8 hour reaction time, the concentration distribution increases. After pores of samples are plugged, the deposition occurs only on the outside surface of samples. The outside surface area is relatively small compared to the

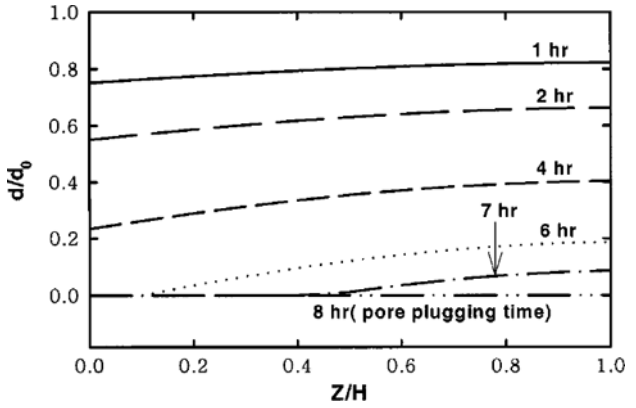

Fig. 4. Changes of dimensionless pore entrance diameter along the axis of cylinder at different reaction times. Reaction conditions: DDS 5%, 10 torr, 20-40 mesh activated carbon, k_r= 10 cm/min.

surface area of pore walls. However, deposition on the outside surface does not give a significant change to the concentration distribution. When the deposit plugs pores of samples, deposition on the pore walls stops, the radius of a sample starts increasing due to deposition on the outside surface. Hence the amount of deposition increases again and the temperature distribution decreases slowly [Xiao et al., 2001; Hinoki et al., 2001].

Fig. 4 is the modeling results of the distribution of pore diameter in the samples along the z-direction.

Pores of samples at the bottom of the reaction zone start plugging at about 6 hr, though pores of samples at the exit of the reaction zone are open yet. These results agree with those in Fig. 3, that the concentration distribution decreases after 8 hr reaction, because pores of all samples in the reactor are plugged at about 8 hr.

Fig. 5 shows changes of the amount of SiC deposition with reaction time at different reaction rate constants. At the time of plugging pores, about 6 or 8 hour, before the amount of deposition with a lower rate constant is more than that with a higher rate constant. This result is due to a relatively uniform concentration distribution in the pores of samples when the rate constant is low. Hence a more

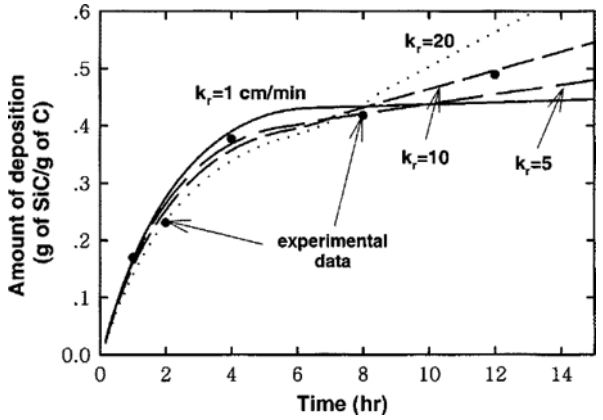

Fig. 5. Changes of the amount of SiC deposition with reaction time at different reaction rate constants. Reaction conditions: DDS 5%, 10 torr, 20-40 mesh activated carbon. Circular symbols are experiment data.

uniform deposition is obtained along the depth of the hole and a greater amount of deposit is resulted. This is one evidence that a lower reaction rate is necessary for a better catalyst support with excellent material properties such as the oxygen resistance, the strength, and the maximum yield, etc. [Hagen, 1999]. However, after the time of plugging pores, the higher rate constant gives a greater amount of deposition because there is no diffusion resistance. Fig. 5 also shows a short plugging time for a higher reaction rate constant.

It is difficult to decide the rate constant by comparing numerical results with the experimental data before the time of plugging pores in Fig. 5, since the differences among lines are not so large. However, by observing the experimental data after the time of plugging pores, it can be concluded that the rate constant is about a value of 10 cm/sec. This result coincides with the reference data [Cho et al., 1996; Chung et al., 1991, 1992; Chung and McCoy, 1991].

2. Effects of the Pressure and the Concentration

Effects of the reaction pressure on the amount of deposition and the surface area are shown in Figs. 6 and 7. The amount of deposi-

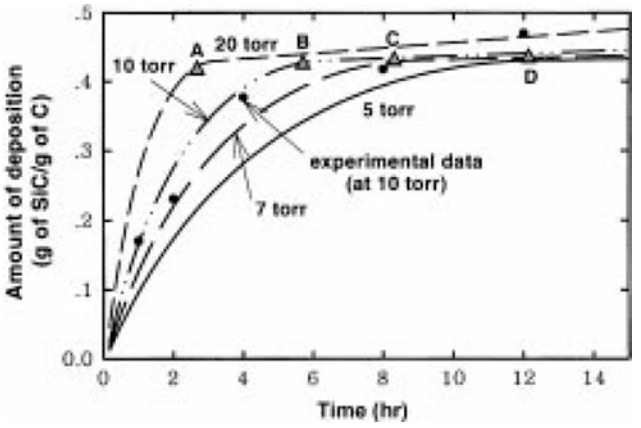

Fig. 6. Changes of the amount of SiC deposition with reaction time at different reaction pressures. Circular symbols are experimental data obtained at 10 torr. Reaction conditions: DDS 5%, 20-40 mesh activated carbon, k_r=10 cm/min.

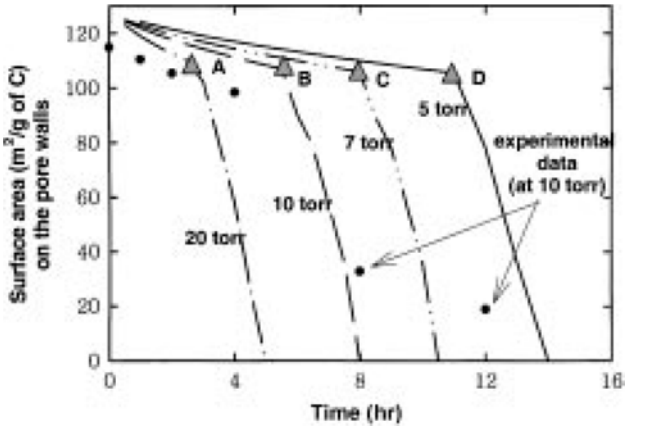

Fig. 7. Changes of the available surface area on the pore walls of activated carbons with reaction time at different reaction pressures. Symbols are experimental data obtained at 10 torr. Reaction conditions: DDS 5% 20-40 mesh activated carbon, k_r=10 cm/min.

tion increases more rapidly at a higher pressure. Here, the high pressure means a high concentration of DDS. So more deposit is obtained and the pore entrance plugs early at a high pressure. The initial parts of the lines in Fig. 6 are due to the deposition on pore walls and the parts after the inflection points are due to the deposition on the outside surfaces of the samples. The inflection points in Fig. 6 are times of plugging pore entrances. At a high pressure, it reaches the inflection point early. However, the final amount of deposition on the pore walls at a higher pressure (point A) is lesser than that at a lower pressure (point D), even though the difference is very small. This is because a more uniform deposition on the pore walls is obtained at a lower pressure. The slope after the inflection point becomes smaller, because the area on the outside surface is smaller compared to the area on the pore walls. The experimental data obtained at 10 torr are similar to the modeling results.

Times of plugging pores of activated carbons could be distinguished easily in Fig. 7. The times are about 14, 10.5, 8, 5 hr at 5, 7, 10, 20 torr, respectively. The plugging time is mainly decided by the concentration at the pore entrance, which is proportional to the pressure. The rapid decrease of the surface area in Fig. 7 is due to the progressive plugging of pores of activated carbons. Pores of activated carbons located at the entrance of the reactor are plugged first and then pores of activated carbons located at the exit are plugged lastly. Here, we can see that the surface areas at the time of plugging pores of activated carbons positioned at the entrance of the reactor (points A, B, C, and D in Fig. 7) is decreasing with the decrease of pressure. This confirms that a more uniform deposition is obtained at a lower pressure. Additionally, in Fig. 7, the slopes of the lines of surface area are decreasing slowly with the decrease of pressure. This also confirms that a more uniform deposition is obtained at a lower pressure.

The experimental data obtained at 10 torr, in Fig. 7, are quite different from the mathematical modeling results, partly because sizes of pore entrances in the real samples are not same as assumed in the mathematical modeling. Hence, pore entrances of activated carbons located at the same axial position in the reactor are not plugged at the same time experimentally. So, even after 12 hr reaction time, there remain open pore entrances as shown in Fig. 7.

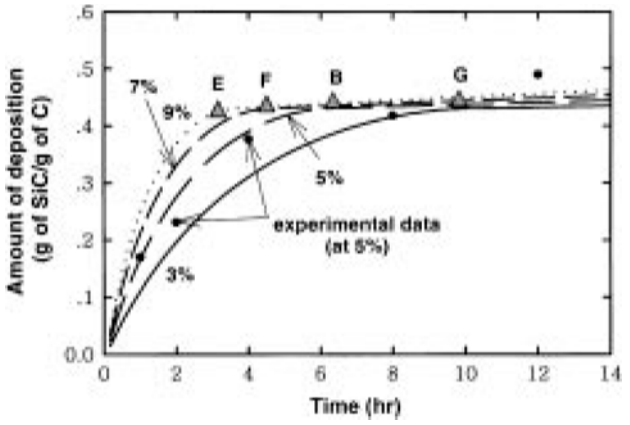

Fig. 8. Changes of the amount of SiC deposit with reaction time at different DDS concentrations. Circular symbols are experimental data obtained at 5% DDS. Reaction conditions: 10 torr, 20-40 mesh activated carbon, k_y = 10 cm/min.

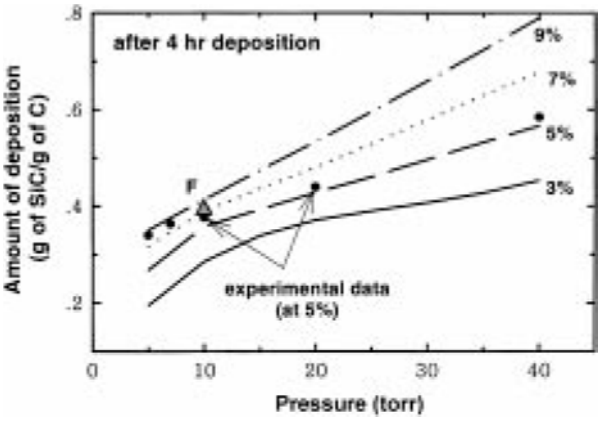

Fig. 9. Changes of the amount of SiC deposit after 4 hr deposition with reaction pressure at different DDS concentrations. Experimental data were obtained at DDS 5%. Reaction conditions: 10 torr, 20-40 mesh activated carbon, k_y = 10 cm/min.

Effects of the concentration are shown in Figs. 8 and 9. As explained before, the amount increases rapidly at first due to the deposition on the pore walls and then increases slowly due to deposition on the outside surfaces of samples [Xu et al., 1999; Yin et al., 2000]. The amount of deposition increases with the increase of concentration. However, the amounts of deposition at the time of plugging pores, points E, F, B, G in Fig. 8, decrease slightly with the increase of the concentration. The experimental data obtained with 5% DDS agree well with the modeling results. Points B in Figs. 6, 7 and 8 are data points at the same time.

Fig. 9 was obtained after 4 hr deposition reaction. From Fig. 8, it can be seen that at 10 torr, when DDS concentrations are 5, 7, 9%, plugging times are near 4 hr. Here, we could confirm that the rate of deposition on pore walls increases with the decrease of DDS concentration. The amounts of deposition are more when the reaction pressure and the concentration are higher. Experimental data are different from modeling results at a low pressure, but agree relatively well at a high pressure.

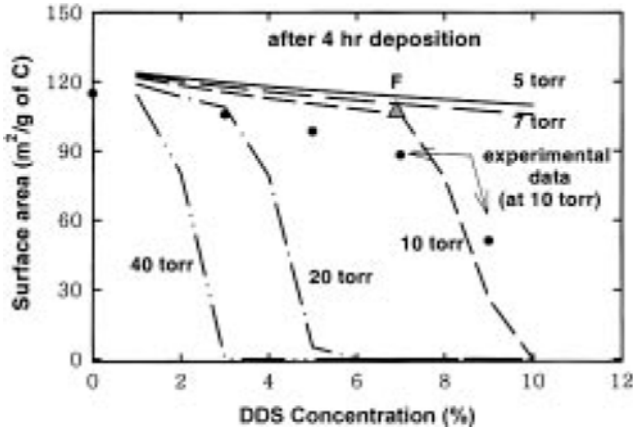

Fig. 10. Changes of the surface area of the sample after 4 hr deposition with DDS concentration at different reaction pressures. Experimental data were obtained at 10 torr. Reaction conditions: DDS 5%, 20-40 mesh activated carbon, k_y = 10 cm/min.

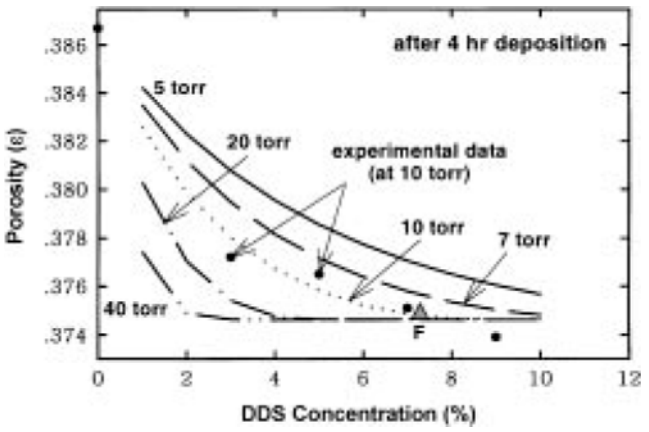

Fig. 11. Changes of the porosity of the sample after 4 hr deposition with DDS concentration at different reaction pressures. Experimental data were obtained at 10 torr. Reaction conditions: DDS 5%, 20-40 mesh activated carbon, k_r = 10 cm/min.

After the 4-hr deposition, surface area and porosity of activated carbons are shown in Figs. 10 and 11. As shown in Fig. 8, with 7% of DDS and the pressure of 10 torr, pores are plugged at about 4 hr (point F). Points F in Figs. 8, 9, 10 and 11 are data points at the same reaction time. From Fig. 10, it can be seen again that more deposition on pore walls is obtained at a lower DDS concentration.

Porosity of 0.374 is the lowest value that can be attained from modeling results. Experimental data changes in the same way as the modeling results.

CONCLUSIONS

Formation of silicon carbide layer on activated carbons of various sizes by CVI in an isothermal fluidized bed reactor was studied and the following conclusions were obtained.

1. In manufacturing of C/SiC composites as a catalyst support, a relatively uniform deposition maintaining a high surface area was obtained at 5 torr of reaction pressure and 3% of DDS concentration. From these results, it was confirmed that, when pressure and concentration are lower, the plugging time of pores would be longer and the catalyst support with a high density and a large surface area would result [Seo et al., 1998].

2. Changes of concentration distribution and sizes of pores of activated carbons were predicted with mathematical modeling. The reaction rate constant of 10 cm/min from references predicted experimental data well.

3. The concentration distribution of DDS in the reactor increases as surface area of activated carbons decreases due to deposition on the pore walls. When pores of activated carbons are plugged, there are only depositions on the outside surface of activated carbons. At this time, the distribution of DDS concentration decreases slowly due to the increase of surface area.

ACKNOWLEDGEMENT

The authors wish to acknowledge financial support from the Korea Science and Engineering Foundation (Grant number: 971-1104-025-2).

NOMENCLATURE

C_A	: mole concentration of DDS in the cylinder [mol/cm^3]
d_0	: diameter of pore entrance of an activated carbon particle [cm]
D_e	: effective diffusion coefficient of DDS [cm^2/min]
D_k	: Knudsen diffusion coefficient [cm^2/min]
D_m	: molecular diffusion coefficient [cm^2/min]
D_{mk}	: composite diffusion coefficient [cm^2/min]
F	: number of activated carbons per unit volume
H	: maximum floating height of activated carbons [cm]
J_A	: diffusion flux of the component DDS [mole/cm^2·sec]
k_r	: first order deposition reaction rate constant [cm/min]
M_m	: molecular weight of deposited SiC [g/mol]
N_A	: mole flux of the component DDS [mole/cm^2·sec]
N_P	: number of pores in an activated carbon
P	: pressure [torr]
R_0	: radius of FB-CVI reactor [cm]
r	: distance in the radial direction of FB-CVI reactor [cm]
r'	: distance in the radial direction of an activated carbon [cm]
r_0	: initial radius of an activated carbon [cm]
r_s	: radius of an activated carbon after plugging time [cm]
q	: number of molecules of Si/SiC generated from a DDS molecule
S	: area per unit volume [cm^2/cm^3 reactor]
T	: temperature [K]
t	: time [min]
v	: linear velocity of the carrier gas [cm/min]
W	: amount of deposition [g/cm^3 reactor]
z	: distance in the direction of gas flow [cm]

Greek Letters

ε	: porosity
ρ_m	: density of deposited material [g/cm^3]
Ω	: surface area of activated carbons per unit volume [cm^2/cm^3]

Subscripts

g	: gas phase
o	: zero time
p	: activated carbon particle
r-, r'-, z-	: r-, r'-, z-direction

REFERENCES

Cho, M. S., Kim, J. W. and Chung, G. Y., "Manufacturing of Ceramic Composites Reinforced with Layered Woven Fabrics by CVI of SiC from Dichlorodimethylsilane," *Korean J. Chem. Eng.*, **13**, 515 (1996).

Chung, G. Y., Cagliostro, D. E., McCoy, B. J. and Smith, J. M., "Rate of Chemical Vapor Deposition of SiC and Si on Single-Layer Woven Fabrics," NASA T.M. (1991).

Chung, G. Y. and McCoy, B. J., "Modelling of Chemical Vapor Infiltration for Ceramic Composites Reinforced with Layered Woven Fab-

rics," *J. Am. Ceram. Soc.*, **74**(4), 746 (1991).
Chung, G. Y., McCoy, B. J., Smith, J. M. and Cagliostro, D. E., "Chemical Vapor Infiltration: Modelling Solid Matrix Deposition for Ceramic Composites with Layered Woven Fabrics," *Chem Engng. Sci.*, **47**(2), 311 (1992).
Hagen, J., "Industrial Catalyst - A Practical Approach," Wiley-VCH, 28-29 (1999).
Hinoki, T., Yang, W., Nozawa, T., Shibayama, T., Katoh, Y. and Kohyama, A., "Improvement of Mechanical Properties of SiC/SiC Composites by Various Surface Treatments of Fibers," *Journal of Nuclear Materials*, **289**, 23 (2001).
Hwang, Y. G. and Chun, H. S., "Enhancement of Mass Transfer in the Fluidized Bed Electrode Reactors," *Korean J. Chem. Eng.*, **16**, 843 (1999).
Kim, Y. M., Song, J. S., Park, S. W. and Lee, J. G., "Nicalon-fiber-reinforced Silicon-Carbide Composites via Polymer Solution Infiltration and Chemical Vapor Infiltration," *J. Mater. Sci.*, **28**, 3866 (1993).
Kobayashi, F., Kawa, K. I. and Iwamoto, K., "Formation of Carbon-excess SiC from Pyrolysis of CH_3SiCl_3," *J. Cryst. Growth*, **28**, 395 (1976).
Naslain, R., "Carbon-ceramic Hybrid Matrix Composites Obtained by Chemical Vapor Infiltration," Proceeding in the 1st Int. Symp. on Functionally Gradient Materials, 71 (1990).
Naslain, R., Hannache, H., Heraud, L., Rossignol, J. Y., Christin, F. and Bernard, C., "Chemical Vapor Infiltration Technique," Proc. 4th European Conf. on Chemical Vapor Deposition, 293 (1983).
Sea, B. K., Choo, S. Y., Lee, T. J., Morooka, S. and Song, S. K., "Tensile Strength and Morphological Investigation of SiC-coated Carbon Fibers," *Korean J. Chem. Eng.*, **12**, 416 (1995).
Seo, G., Kim, T. J., Lim, S., Ko, C. H. and Ryoo, R., "The Reduction of Dissolved Oxygen by Hydrazine over Platinum Catalyst Supported on Disordered Mesoporous Materials," *Korean J. Chem. Eng.*, **15**, 611 (1998).
Sugiyama, K. and Kurisu, Y., "Reinforcement and Antioxidizing of Porous Carbon by Pulse-CVI of SiC," *J. Mater. Sic.*, **24**, 3756 (1989).
Van den Brekel, Fonville, R. M. M., van der Straten, P. J. M. and Verspui, G., "CVD of Ni, TiN and TiC on Complex Shapes," *Proc. Electrochem. Soc.*, **81**, 142 (1981).
Xiao P., Xu, Y. D., Zhang, L. T., Cheng, L. F. and Chen, Z. F., "Continuous Synchronous Composite Process for Fabricating Carbon/Silicon Carbide Composites," *Materials Science and Engineering*, **A313**, 244 (2001).
Xu, Y., Cheng, L. and Zhang, L., "Carbon/Silicon Carbide Composites Prepared by Chemical Vapor Infiltration Combined with Silicon Melt Infiltration," *Carbon*, **37**, 1179 (1999).
Yin, X., Cheng, L., Zhang, L., Xu, Y. and You, C., "Microstructure and Oxidation Resistance of Carbon/Silicon Carbide Composites Infiltrated with Chromium Silicide," *Materials Science and Engineering*, **A290**, 89 (2000).